



## Double Population MRT Lattice Boltzmann Method in an Enclosure Using Nanofluid

Farzaneh Bakhtvar<sup>1</sup>, Nor Azwadi Che Sidik<sup>1,\*</sup>

<sup>1</sup> Faculty of Engineering, Universiti Teknologi Malaysia, 81310 Skudai, Johor, Malaysia

### ARTICLE INFO

#### Article history:

Received 1 March 2022

Received in revised form 2 June 2022

Accepted 15 June 2022

Available online 27 June 2022

#### Keywords:

Lattice Boltzmann method; nanofluid;  
Rayleigh number

### ABSTRACT

In this study, lattice Boltzmann method was applied to investigate the natural convection flows utilizing nanofluids in a square enclosure.  $Al_2O_3$  and CuO water based nanofluids with 5, 6, 7, 8 and 9 % nanoparticle volume fraction were used as the fluid. This study has been carried out for the pertinent parameters in the following ranges: the Rayleigh number of nanofluid,  $Ra=103, 104, 105$  and  $106$ , the volumetric fraction of nanoparticles 5, 6, 7, 8 and 9 % and the aspect ratio ( $Ar$ ) of the enclosure is 1.0. The effects of solid volume fraction of nanofluids on hydrodynamic and thermal characteristics were investigated and discussed. The average and local Nusselt numbers, streamlines, temperature contours and vertical component of velocity for different values of solid volume fraction and Rayleigh number are then illustrated. Results show that by increasing Rayleigh number and nanoparticle volume fraction, average Nusselt number increases in whole range of Rayleigh numbers that lead to decreasing thermal boundary layer and enhancement of heat transfer of fluid in the cavity. As expected,  $Al_2O_3$  with higher heat conductivity has higher Nusselt number with respect to CuO with lower heat conductivity.

## 1. Introduction

In the last century, Computational Fluid Dynamic (CFD) had been widely used due to advancement in computation technology. Basically, CFD has been used and compared the solution between the experiment results and analytical results [1]. In addition, CFD also helps to interpret as well as to study the behaviour of fluids. Although CFD is a powerful tool to demonstrate the fluid flow behaviour, however the error gain in the simulations is still an issue that needs great attention from researcher. Besides that, Casalino *et al.*, [2] discovered that the conventional CFD is difficult in solving multi-phase flow due to complexity of the partial differential equation. In most of the cases, Navier-Stokes (NS) equation becomes the fundamental basic for CFD in simulating fluid flow. Rather than NS equation, CFD also has been used to solve the continuity equation, the energy equation and other equation which are derived from equation mention before [3]. There are many types of numerical approaches that can be chosen to solve all kind of these equation in order to solve the fluid problems.

In 1990's, a new CFD method was introduced to solve complex system tools which historically it's originated from lattice gas automata (LGA). This method is based on mesoscopic numerical approach

\* Corresponding author.

E-mail address: [azwadi@utm.my](mailto:azwadi@utm.my)

which is something between macroscopic (FDM, FVM, FEM...) and microscopic method and is suitable for solving each fluid dynamic and either system related to partial differential equations [4].

In this method, fluids can be simulated by modelling of its individual molecules that are consistent. So, it will behave as a fluid if all the interactions between molecules can be calculated correctly. But simulating such a fluid with this much numbers of molecules need a huge amount of data that should be calculated by computers. It's the biggest disadvantage of such a method that computer resources are not prepared with. In fact, lattice Boltzmann method (LBM) is a bridge between molecular description that defines as kinetic of fluid motion and the real macroscopic world [5]. The kinetic theory tries to understand the macroscopic properties of fluids from the properties of their molecules which include molecular mass, electrical properties shape parameters, the mean free path and so on [6,7].

Recently, the lattice Boltzmann equation (LBE) method has gained much attention for its ability to simulate fluid flows, and for its potential advantages over conventional numerical solution of the NS equations [8]. A few standard, benchmark problems have been simulated by LBE and the results were shown to agree quite well with the corresponding NS solutions. Currently, a number of other complex flow problems are being simulated using the LBE approach.

LBM has several advantages compared to traditional CFD method especially when solving the complex boundaries problems. Most of the CFD methods are time consuming, but LBM can save a lot of time due to its flexibility on boundary treatment. This is because LBM only calculates due to its number of mesh points and the lattice model rather than calculate random motion of every particle. After LBM has been introduced for many years, it already shows its high capability in simulating the behaviour of flow in macroscopic channel. Most of the results obtained from LBM are in good agreement with analytical results and other numerical results. The flow pattern and its behaviour can be studied through analyzing the outcome of results [9].

The LBM uses ensemble averaged distribution function to describe the kinetic system and considers that the collective behaviour of the imagined particles which characterize the system, is in agreement by the principle of macroscopic physics. Nowadays the LBM has established itself as a powerful tool for the simulation of a wide range of physical phenomena. One of its main applications is the field of CFD where it has proven successful to solve the weakly compressible NS equations and models associated with more complex flows involving several phases or components. It has also been successfully applied to the simulation of flows of pseudo plastic and viscoelastic fluids. This method does not solve directly the macroscopic conservation equations, but somewhat models the statistics of collision of particles and may offer more modeling freedom than the classical methods based on finite difference, finite volume or finite element to which it is a competitive alternative.

Considering the rapid pace with which the subject is developing, in the foreseeable future the LBE method is likely to play a significant role in the numerical prediction of flows. A particularly simple linearized version of the collision operator makes use of a relaxation time towards an equilibrium value using a single relaxation time parameter. The relaxation term is known as the Bhatnagar–Gross–Krook (BGK) collision operator [10]. This model is called the lattice Boltzmann BGK model. Use of this collision operator makes the computations much faster. Due to the extreme simplicity, the lattice BGK (LBGK) equation [11-15] has become the most popular LBM.

Partial differential equation presents fluid flow through the space and time. As a matter of fact, certain solutions only exist for a few specific cases with simple geometries and suitable boundary conditions. It is certainly true that to obtain simplified equation; the complex phenomena must be ignored. However, nowadays digital computers have been rapidly developed and many researchers prefer to use high performance computers in their field of study.

The properties of water-based nanofluids have been presented in the form of tables or equations and heat transfer effects is investigated because the demand on usage of nanofluids is rapidly increasing but research on the nanofluids still has a big gap between numerical and experimental results. Also, behaviour of nanofluids is not well understood so in this study we tried to investigate different factors which affects the heat transfer conditions of different nanofluids to find the best aspect ratio and volume fraction of each nanofluid to have the best heat transfer in a square cavity.

## 2. Methodology

### 2.1 Lattice Boltzmann Method (LBM) for Fluid Flow

LBM is a relatively new simulation technique for complex fluid systems and has attracted interest from researchers in computational physics. Unlike the traditional CFD methods, which solve the conservation equations of macroscopic properties (i.e., mass, momentum and energy) numerically, LBM models the fluid consisting of fictive particles, and such particles perform consecutive propagation and collision processes over a discrete lattice mesh. Due to its particulate nature and local dynamics, LBM has several advantages over other conventional CFD methods especially in dealing with complex boundaries, incorporating of microscopic interactions and parallelization of the algorithm. A different interpretation of the LBE is that of a discrete-velocity Boltzmann equation. The numerical methods of solution of the system of partial differential equations then gives rise to a discrete map, which can be interpreted as the propagation and collision of fictitious particles.

The D2Q9 LBM model was used to simulate fluid flow in 2D channel with uniform grid size of  $\delta x$  by  $\delta y$ . The LBE (known as LBGK equation) with single relaxation time can be expressed as in Eq. (1) and (2),

$$f_i(\vec{r} + \delta t \vec{c}_i, t + \delta t) - f_i(\vec{r}, t) = -\frac{1}{\tau_f} (f_i(\vec{r}, t) - f_i^{eq}(\vec{r}, t)) \quad (1)$$

which can be reformulated as,

$$f_i(\vec{r} + \delta t \vec{c}_i, t + \delta t) = \omega_f f_i^{eq}(\vec{r}, t) + (1 - \omega_f) f_i(\vec{r}, t) \quad (2)$$

where,  $\omega_f = \frac{1}{\tau_f}$ , and  $\tau_f$  the single relaxation time of the fluid,  $f_i$  represents the particle distribution function,  $e_i$  is the particle streaming velocity and  $f_i^{eq}$  is the local equilibrium distribution function. For D2Q9 model  $f_i^{eq}$  is given by Eq. (3),

$$f_i^{eq} = \rho \omega_i \left[ 1 + 3e_i u + \frac{9}{2} (e_i \cdot u)^2 - \frac{3}{2} u^2 \right] \quad (3)$$

where,  $\rho$  is the density of the fluid and  $\omega_i$  is the weight function, which has the values of  $\omega_0 = \frac{1}{9}$ ,  $\omega_i = \frac{1}{9}$  for  $i = 1$  to 4,  $\omega_i = \frac{1}{36}$  for  $i = 5$  to 8. The macroscopic fluid flow velocity in lattice units is represented by  $u$ . in the LBM, the fluid macroscopic quantities such as density,  $\rho$ , and flow momentum,  $\rho u$ , are calculated by using the distribution function  $f_i$ , and given by  $\rho = \sum_{i=0}^N f_i$  and  $\rho u = \sum_{i=0}^N \vec{e}_i f_i$  respectively. The streaming speed for particles in coordinates (X and Y) directions can be expressed as  $e_i = \cos\left(\frac{\pi}{2}(i-1)\right)$  and  $\sin\left(\frac{\pi}{2}(i-1)\right)$ , whereas particles in diagonal directions have velocities of

$e_i = \sqrt{2} \left( \cos\left(\frac{\pi}{4}(2i - 9)\right), \sqrt{2} \left( \sin\left(\frac{\pi}{4}(2i - 9)\right) \right) \right)$ , however, the particle in the lattice center is at rest and has no streaming speed; i.e.  $e=0$ .

The thermal part is simulated by using another distribution function for the temperature. For instance,  $g$  is used to simulate the distribution function of the dependent variable (temperature) in the LBE and an approach similar to that used to simulate the fluid flow is utilized to simulate the temperature distribution. In addition, the algorithm suggested by Kamyar *et al.*, [13], is adopted throughout this work.

The kinetic equation for the temperature distribution function with single relaxation time is given by,

$$\frac{\partial g_i}{\partial t} + e_i \nabla g_i = -\frac{1}{\tau_t} (g_i - g_i^{eq}) \quad (4)$$

which can be written in the form,

$$g_i(\vec{r} + \delta t \vec{e}_i, t + \delta t) = \omega_t g_i^{eq}(\vec{r}, t) + (1 - \omega_t) g_i(\vec{r}, t) \quad (5)$$

where,  $g_i$  represents the temperature distribution function of the particles,  $g_i^{eq}$  is the local equilibrium distribution function of the temperature and  $w_t = \frac{1}{\tau_t}$  where  $\tau_t$  is the single relaxation time of the temperature distribution. Thus, the equilibrium distribution function of the thermal part is given by Kamyar *et al.*, [13],

$$g_i^{eq}(r, t) = \phi(r, t) \omega_i \left[ 1 + \frac{e_i \cdot u}{c_s^2} \right] \quad (6)$$

where,  $\phi$  is the macroscopic temperature and  $c_s^2$  is the speed of sound. The diffusion coefficient can be obtained as a function of the relaxation time and given by  $= \frac{\Delta r^2}{\Delta t D} \left( \frac{1}{\omega} - \frac{1}{2} \right)$  the macroscopic temperature is then computed from,

$$\phi(r, t) = \sum_{i=0}^{N-1} g_i(r, t) = \sum_{i=0}^{N-1} g_i^{eq}(r, t) \quad (7)$$

A uniform lattice of  $128 \times 128$  was used to perform all of the simulations. However, the number of lattices was doubled to test the grid dependency results.

## 2.2 Geometry

The geometry used in this study consist of a 2D square cavity (Figure 1) of height, H and weight, W. Left wall is the hot wall and right wall is the cold wall and top and bottom walls were assumed to be adiabatic and also no conduction was considered in the walls. The aspect ratio of the geometry was defined as the ratio of weight of enclosure to the height ( $Ar=W/H$ ). Inside the cavity was filled with nanofluid and the buoyancy force is the only external force acting on the fluid.

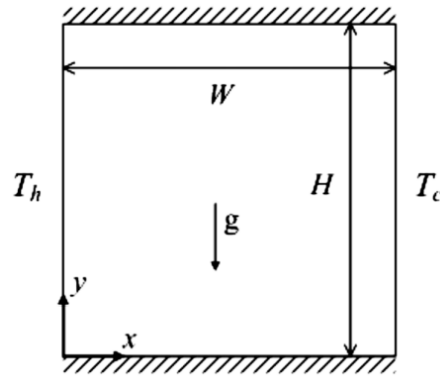
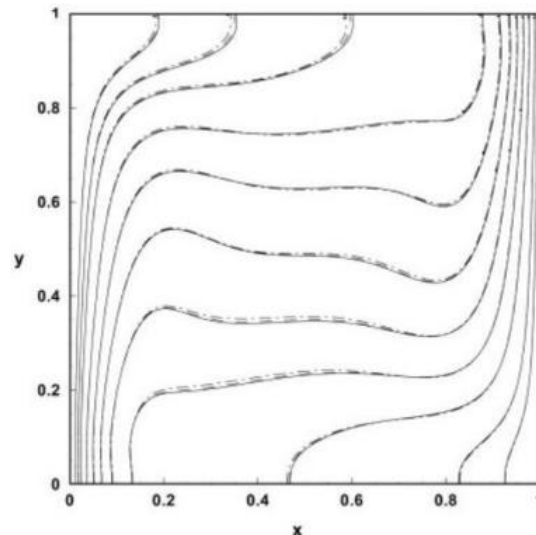


**Fig. 1.** Schematic domain of the physical model

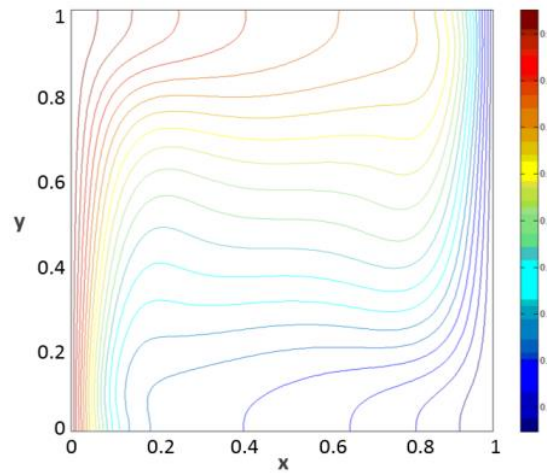
### 3. Results and Discussion

#### 3.1 Code Validation

To validate the numerical simulation, the results of natural convection in square cavity were compared with previous works [14]. At the square cavity, an assumption was made that the initial stationary flow was heated from the left wall, while the right wall was maintained at a constant low temperature. Meanwhile, the upper and bottom boundary walls were assigned adiabatic boundary conditions (Figure 2 and 3). A vertical gravitational effect was applied in the  $y$ -direction. Regarding the flow field, the square cavity was assumed to be closed and the non-slip boundary conditions were imposed at each of the four solid walls.

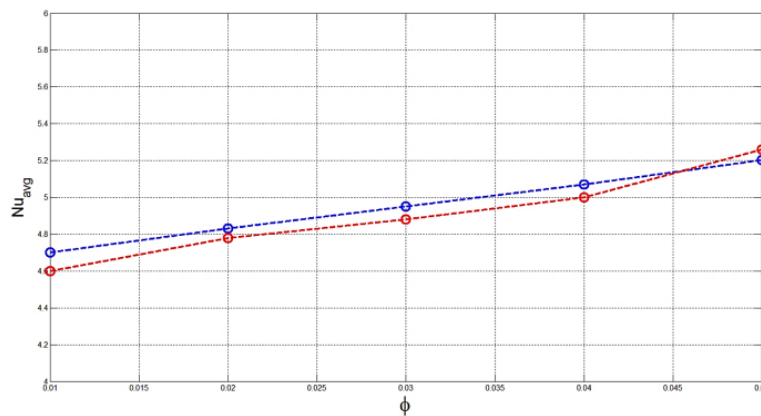


**Fig. 2.** Isotherms for Cu–water nanofluid at  $Ra = 10^5$  and 5 % volume fraction



**Fig. 3.** Isotherms for Cu-water nanofluid at  $Ra = 10^5$  and 5% volume fraction MRT-SRT LBM

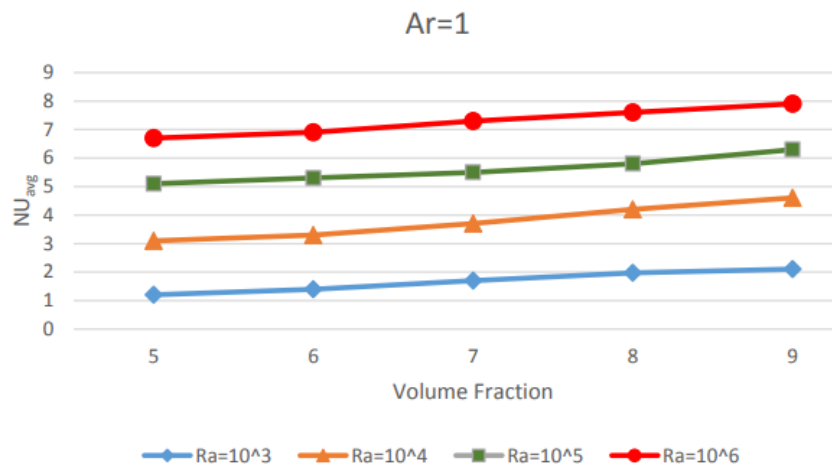
The results of the present study both isotherms and average Nusselt numbers show a good agreement with the previous study (Figure 4).



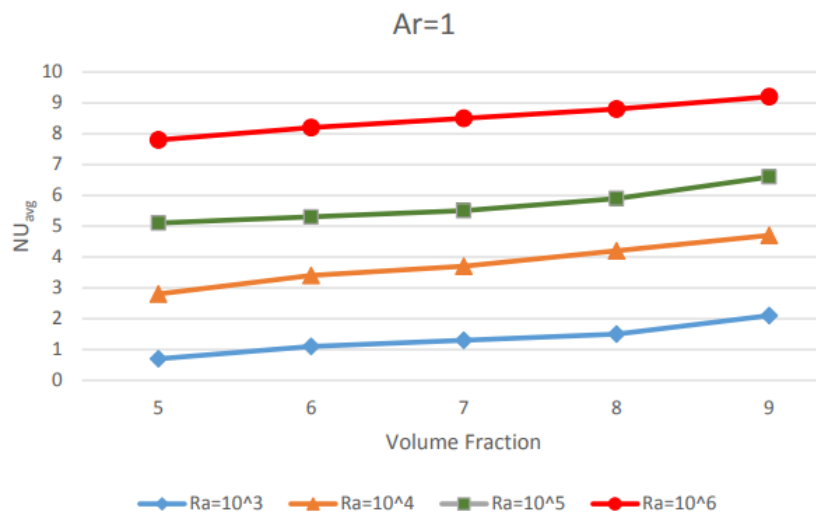
**Fig. 4.** Nusselt and volume fraction from 1 - 5% Rayleigh  $10^5$

### 3.2 Effect of Volume Fraction

Figure 5 and 6 show changes of Nusselt average by changing volume fraction of the nanofluid for all the Rayleigh numbers in  $Al_2O_3$  and  $CuO$  nanoparticles respectively. As these graphs show increase of volume fraction of nanoparticles that led to increase in Nusselt average.



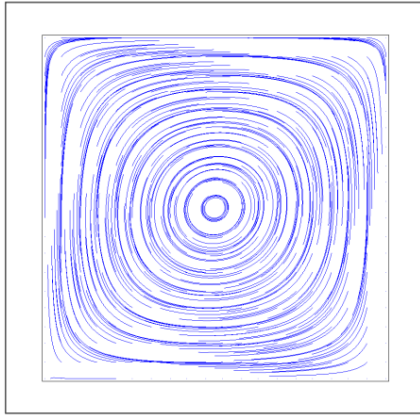
**Fig. 5.** Changing Nusselt average with volume fraction for Al<sub>2</sub>O<sub>3</sub> nanoparticles



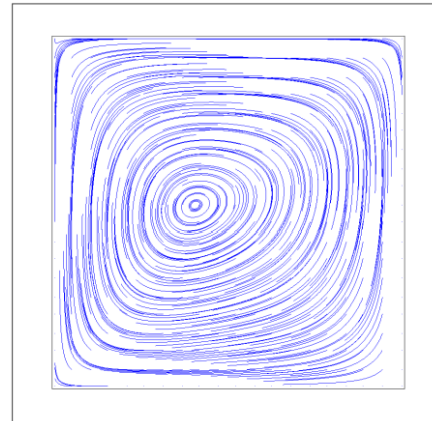
**Fig. 6.** Changing Nusselt average with volume fraction for CuO nanoparticles

Figure 7 - 11 illustrates comparisons of the streamlines and isotherms of Al<sub>2</sub>O<sub>3</sub>/Water nanofluid at Rayleigh number of 10<sup>3</sup>, 10<sup>4</sup>, 10<sup>5</sup> and 10<sup>6</sup>. The strength of circulation increases with an increasing particle volume fraction at a particular Rayleigh number. For a low Ra flow, the isotherm was almost vertical since heat is transferred by conduction between the hot and cold walls. However, the heat transfer mechanism changes from conduction to convection as Ra increases. The thickness of thermal boundary layer near the wall decreases with the increase of Ra and the isotherm at the centre of the cavity becomes horizontal while it is vertical only within the thin boundary layers. In addition, with the use of a nanofluid, the lesser temperature gradient at the heated surface compared to the use of pure water due to the growth of thermal boundary thickness was revealed. It is found to have a negative influence on Nu. However, since the effect of the ratio of nanofluid conductivity to water conductivity,  $k_{nf}/k_{bf}$  is more pronounced than the effect of temperature gradient, an enhancement of Nu was observed with a nanofluid in the following discussions. To compare the effect of volume fraction on the streamlines, the aspect ratio is considered constant for Al<sub>2</sub>O<sub>3</sub> nanofluid and the Rayleigh number and volume fraction is changed. As these graphs show, increasing volume fraction causes change in streamline that tends to move toward the walls.

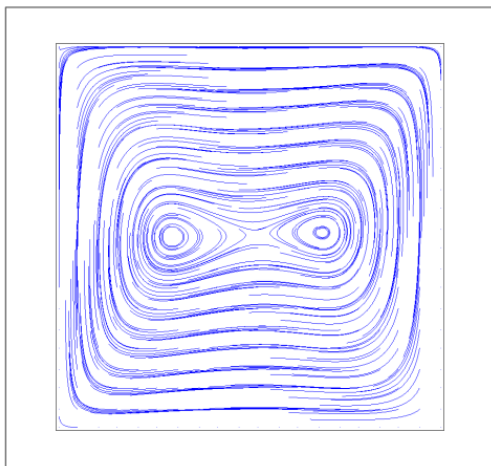




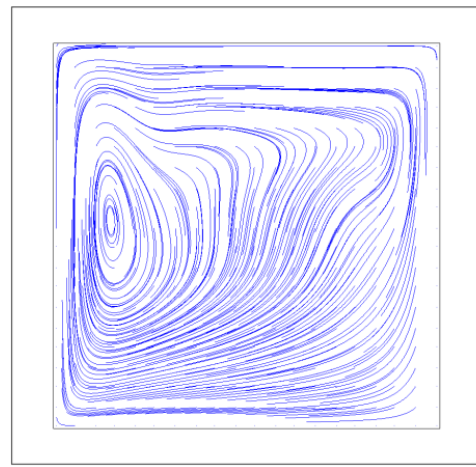
**Fig. 7.**  $Ra=10^3$ , Volume fraction 9 % for  $Al_2O_3$ /Water nanofluid



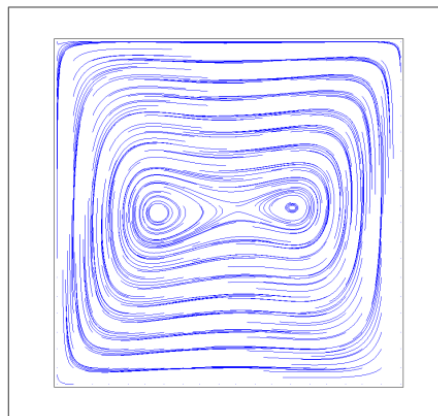
**Fig. 8.**  $Ra=10^4$ , Volume fraction 9 % for  $Al_2O_3$ /Water nanofluid



**Fig. 9.**  $Ra=10^5$ , Volume fraction 9 % for  $Al_2O_3$ /Water nanofluid



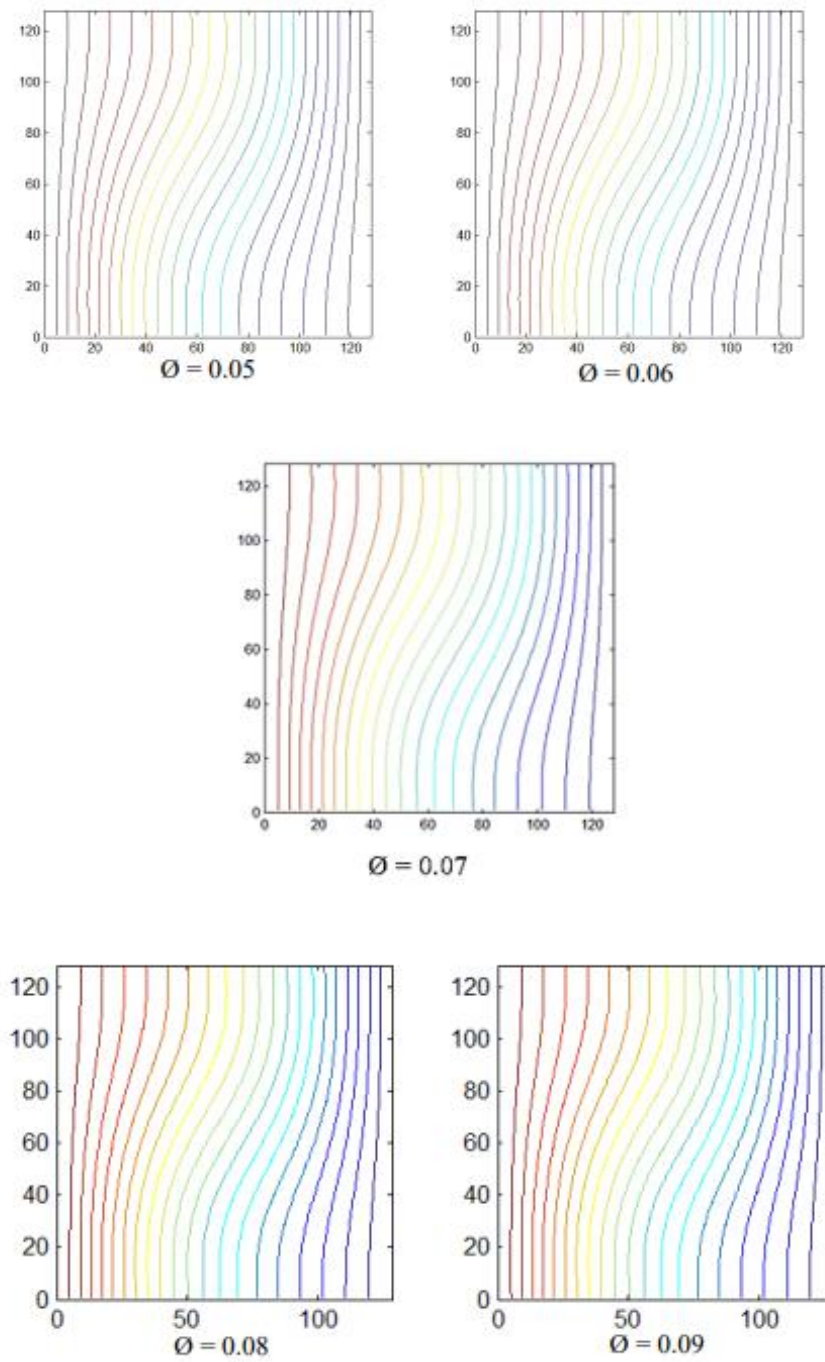
**Fig. 10.**  $Ra=10^6$ , Volume fraction 9 % for  $Al_2O_3$ /Water nanofluid



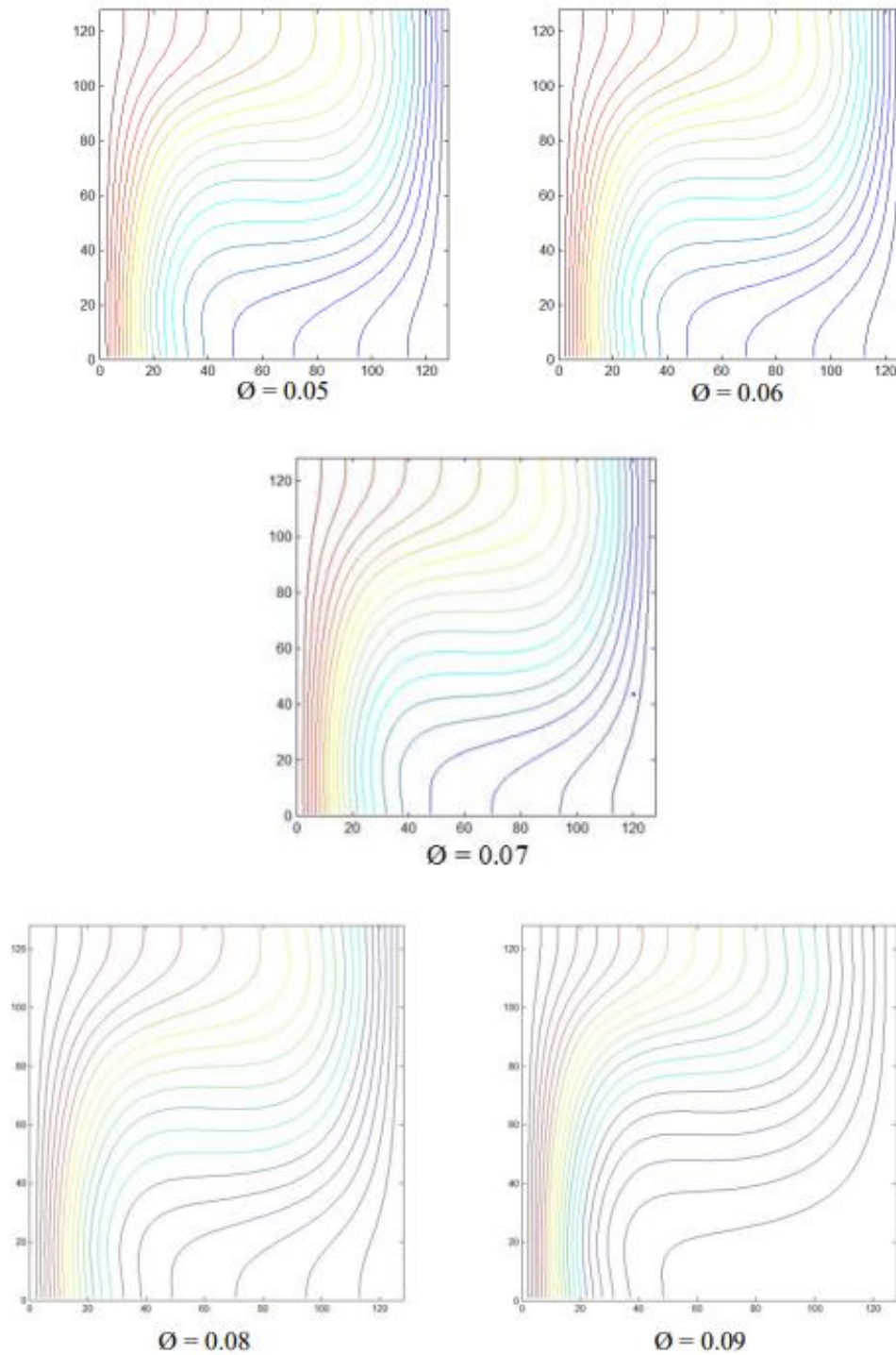
**Fig. 11.**  $Ra=10^5$ , Volume fraction 9 % for CuO/Water nanofluid

The effect of volume fraction on temperature field is shown in Figure 12 for  $Ra=10^3$ , Figure 13 for  $Ra=10^4$  and in Figure 14 for  $Ra=10^5$  in different volume fractions in aspect ratio 1.0 of  $Al_2O_3$  nanoparticles. The figures show that the thickness of thermal boundary layer decreases by increasing the volume fraction. It is due to the increasing conduction heat transfer associated with presence of the nanofluid, so this effect is higher in  $Al_2O_3$  nanoparticles because of its higher thermal conductivity.

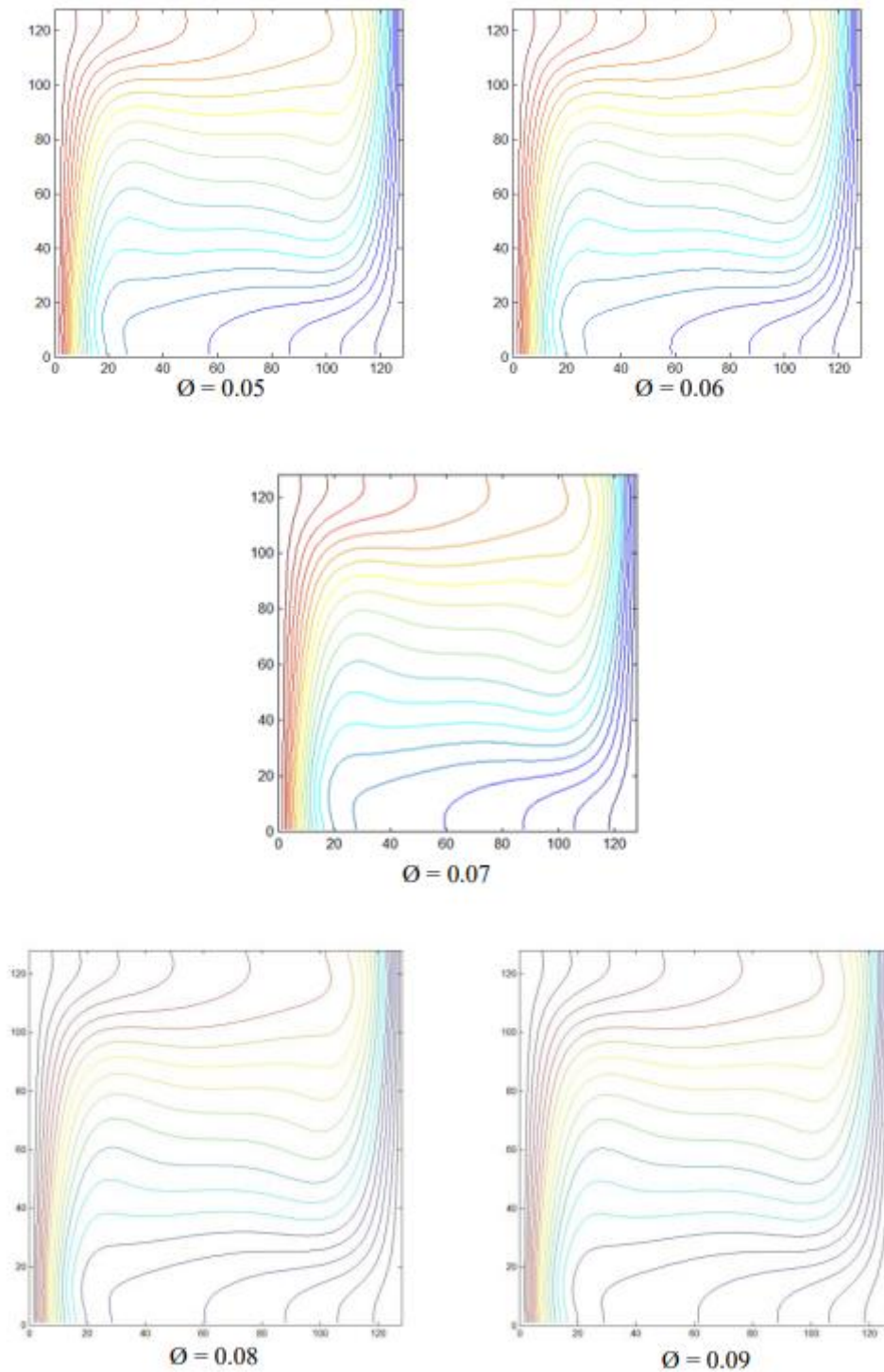




**Fig. 12.** Isotherms for  $\text{Al}_2\text{O}_3$ -water nanofluid at  $\text{Ra} = 10^3$ ,  $\phi = 0.05 - 0.09$

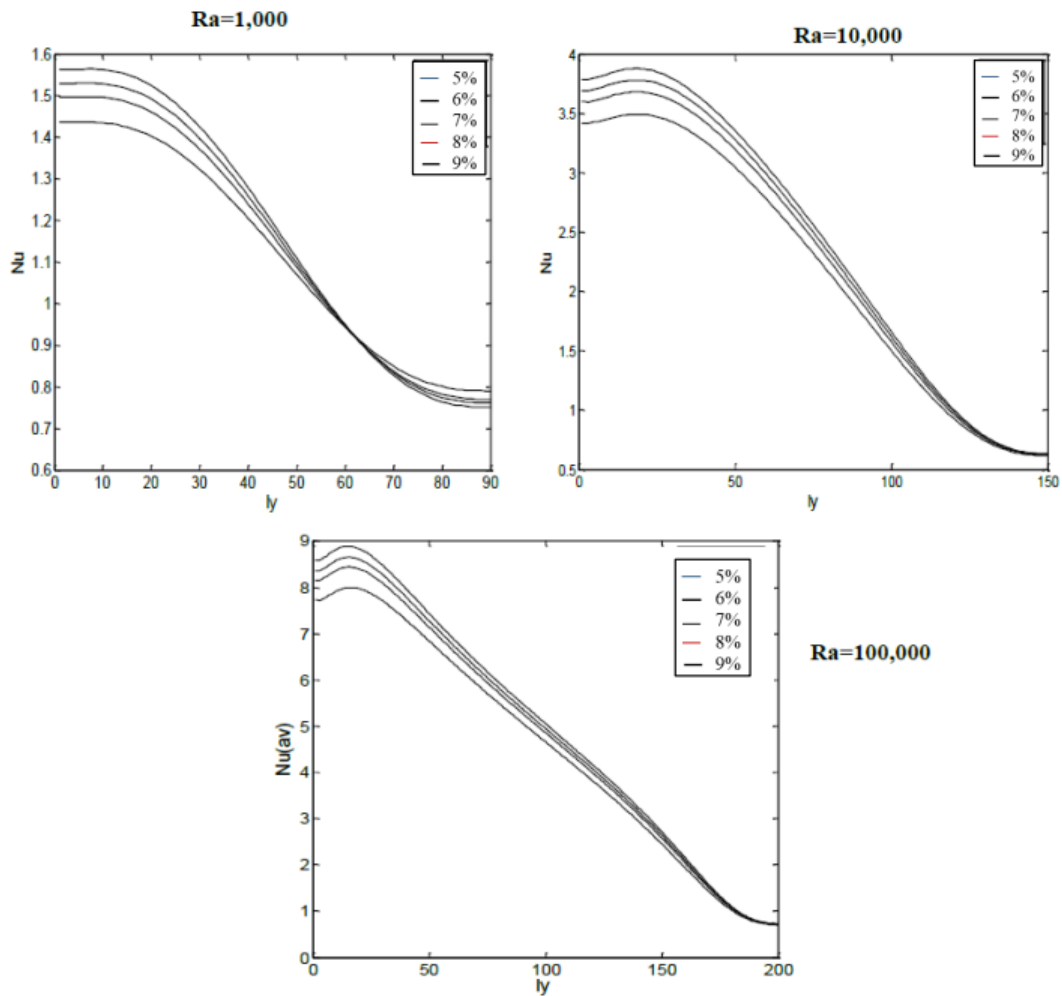


**Fig. 13.** Isotherms for  $\text{Al}_2\text{O}_3$ -water nanofluid at  $\text{Ra} = 10^4$ ,  $\phi = 0.05 - 0.09$



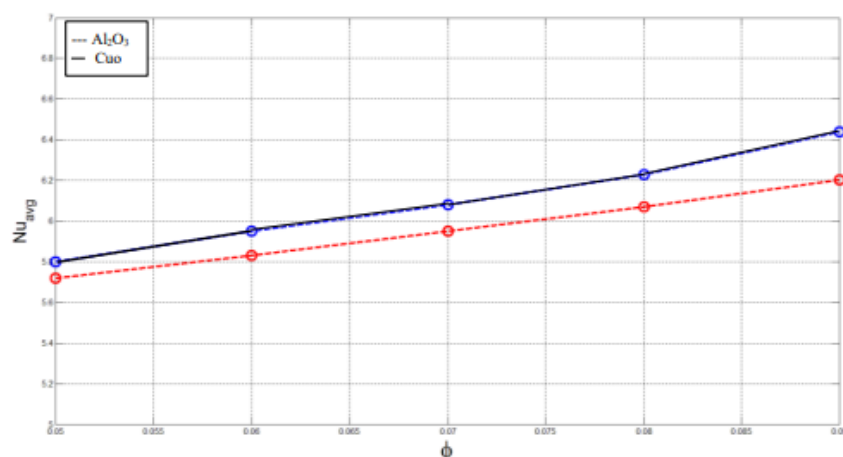
**Fig. 14.** Isotherms for  $\text{Al}_2\text{O}_3$ -water nanofluid at  $Ra = 10^5$ ,  $\phi = 0.05 - 0.09$

Figure 15 illustrates how the addition of nanoparticles influences the Nusselt number distribution along the heated surface for three different  $Ra$  numbers. It is evident that increasing the volume fraction increases the  $Nu$  number particularly close to the bottom of the hot wall for both nanoparticles. It can be observed that the effect of  $\text{Al}_2\text{O}_3$  nanoparticles was in comparison to the  $\text{CuO}$ . This is due to a number of effects such as Brownian motion, ballistic phonon transport, layering at the solid/liquid interface and dispersion effect.



**Fig. 15.** Effect of volume fraction on local Nusselt number across heated wall

In Figure 16 the effect of volume fraction on Nusselt number for  $\text{Al}_2\text{O}_3$  and  $\text{CuO}$  nanoparticles are shown for  $\text{Ra}=10^5$  and as it shows, the average Nusselt number of both nanofluids increased by increment of the nanoparticle volume fraction.



**Fig. 16.** Average Nusselt number for  $\text{Al}_2\text{O}_3$ -water nanofluid and  $\text{CuO}$ -water nanofluid for  $\text{Ra}=10^5$  and volume fractions from 5 - 9 %

### 3.3 Effect of Rayleigh Number

Figure 17 and 18 show a comparison of the isotherm contours between the nanofluids at  $\phi=0.05$  and the basefluid for three various Rayleigh numbers for  $\text{Al}_2\text{O}_3$  and  $\text{CuO}$ . The nanofluid isotherms become closer to the vertical walls and are more uniformly distributed in the core region of the enclosure at different aspect ratios. Also, in the case of  $\text{Ra}=10^3$  and aspect ratio  $\text{Ar}=1.0$ , the isotherms become almost parallel to the heated wall. The isotherms exhibit a trend almost similar to conduction in solids. This behaviour leads to an enhancement in heat transfer for  $\gamma>1/2$ .

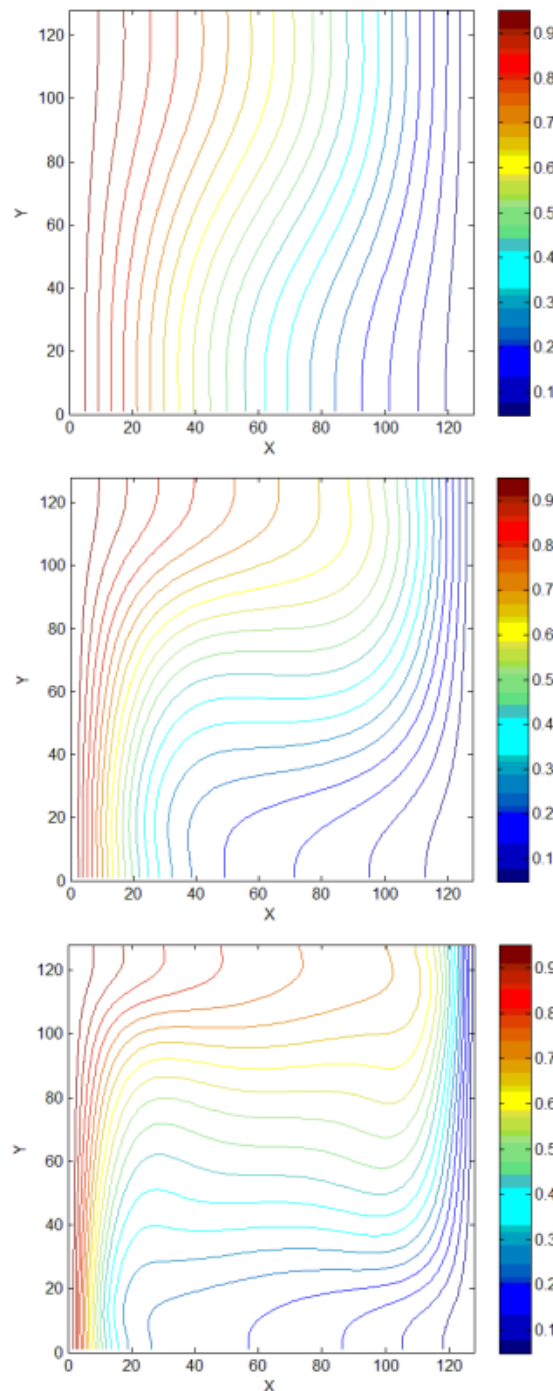


**Fig. 17.** Comparison of isotherms by changing Rayleigh number for  $\text{Al}_2\text{O}_3$ ,  $\phi=5\%$  for  $\text{Ra}=10^3, 10^4$  and  $10^5$

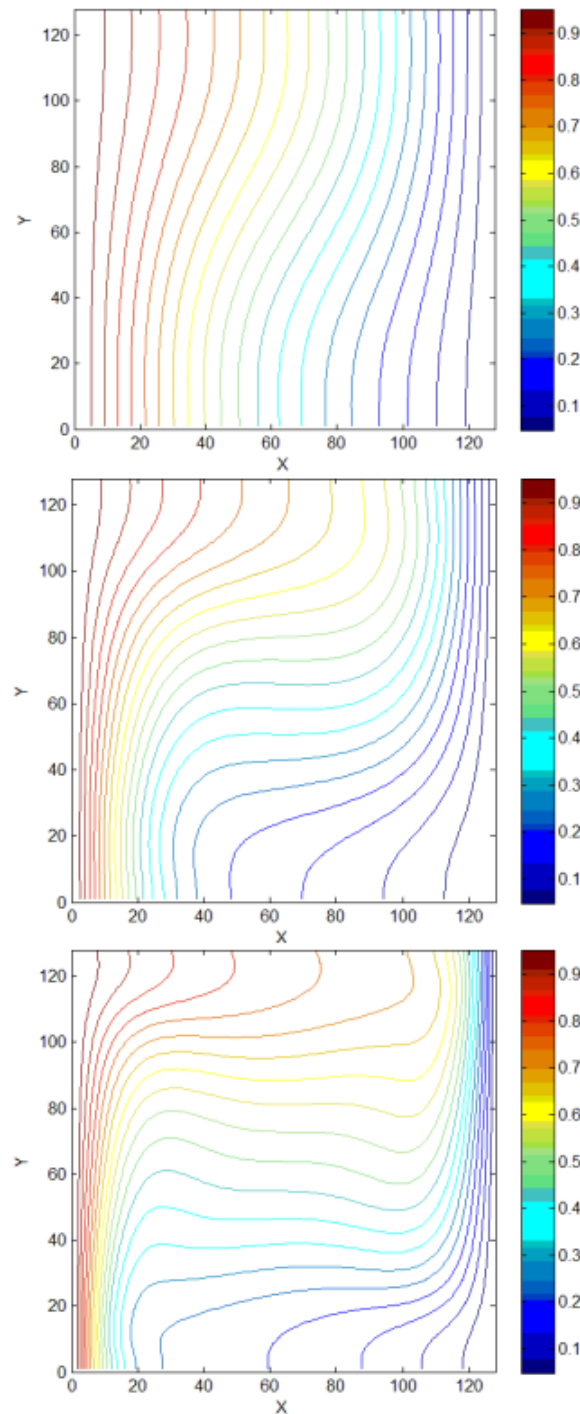


**Fig. 18.** Comparison of isotherms by changing Rayleigh number for CuO,  $\phi=5\%$  for  $Ra= 10^3, 10^4$  and  $10^5$

#### 4. Conclusion

Heat transfer enhancement in a square enclosure subjected to different side wall temperatures using nanofluid was studied by MRT-SRT LBM. The results are presented at different Rayleigh numbers, volume fractions and CuO/water and Al<sub>2</sub>O<sub>3</sub>/water nanofluids. It is found that the LBM is a suitable approach for simulating nanofluid. The simple implementation of effective thermal conductivity was the most advantages of this method. The most important advantage of this method



was simplicity in simulation of nanofluid behaviour in comparison with other computational fluid method. Below are other conclusions obtained from this research.

- i. With increasing the solid volume fraction, the results show a heat transfer enhancement at any Rayleigh number.
- ii. Heat transfer enhances with increase in Rayleigh number for a particular volume fraction.
- iii. The CuO/water nanofluids exhibit higher heat transfer rates than Al<sub>2</sub>O<sub>3</sub>/water at a given Rayleigh number, as also revealed in many published numerical studies. The reason might be that due to a significant increase in effective dynamic viscosity compared to that of the base fluid, a larger temperature difference across the square cavity was specified to drive a nanofluid and consequently a stronger convection was induced, which results in a larger Nu using the Al<sub>2</sub>O<sub>3</sub> nanofluid.
- iv. The results illustrate that the types of nanofluid is a key factor for heat transfer enhancement and the highest and lowest values of Nu number were obtained when using Al<sub>2</sub>O<sub>3</sub> and CuO nanoparticles respectively.

## References

- [1] Bhatti, Muhammad Mubashir, M. Marin, Ahmed Zeeshan, and Sara I. Abdelsalam. "Recent trends in computational fluid dynamics." *Frontiers in Physics* 8 (2020): 593111. <https://doi.org/10.3389/fphy.2020.593111>
- [2] Casalino, Damiano, Gianluca Romani, Raoyang Zhang, and Hudong Chen. "Lattice-Boltzmann calculations of rotor aeroacoustics in transitional boundary layer regime." *Aerospace Science and Technology* 130 (2022): 107953. <https://doi.org/10.1016/j.ast.2022.107953>
- [3] Zawawi, Mohd Hafiz, A. Saleha, A. Salwa, N. H. Hassan, Nazirul Mubin Zahari, Mohd Zakwan Ramli, and Zakaria Che Muda. "A review: Fundamentals of computational fluid dynamics (CFD)." In *AIP conference proceedings*, vol. 2030, no. 1. AIP Publishing, 2018. <https://doi.org/10.1063/1.5066893>
- [4] Yan, Bo, and Guangwu Yan. "A steady-state lattice Boltzmann model for incompressible flows." *Computers & Mathematics with Applications* 61, no. 5 (2011): 1348-1354. Succi, Sauro, and S. Succi. *The lattice Boltzmann equation: for complex states of flowing matter*. Oxford university press, 2018. <https://doi.org/10.1016/j.camwa.2010.12.078>
- [5] Norman, Patrick, Kenneth Ruud, and Trond Sæue. *Principles and practices of molecular properties: Theory, modeling, and simulations*. John Wiley & Sons, 2018. <https://doi.org/10.1002/9781118794821>
- [6] Chandran, Sivasurender, Jörg Baschnagel, Daniele Cangialosi, Koji Fukao, Emmanouil Glynos, Liesbeth MC Janssen, Marcus Müller et al. "Processing pathways decide polymer properties at the molecular level." *Macromolecules* 52, no. 19 (2019): 7146-7156. <https://doi.org/10.1021/acs.macromol.9b01195>
- [7] Sharma, Keerti Vardhan, Robert Straka, and Frederico Wanderley Tavares. "Lattice Boltzmann methods for industrial applications." *Industrial & Engineering Chemistry Research* 58, no. 36 (2019): 16205-16234. <https://doi.org/10.1021/acs.iecr.9b02008>
- [8] Afrouzi, Hamid Hassanzadeh, Majid Ahmadian, Mirollah Hosseini, Hossein Arasteh, Davood Toghraie, and Sara Rostami. "Simulation of blood flow in arteries with aneurysm: Lattice Boltzmann Approach (LBM)." *Computer methods and programs in biomedicine* 187 (2020): 105312. <https://doi.org/10.1016/j.cmpb.2019.105312>
- [9] Shan, Xiaowen, Xuhui Li, and Yangyang Shi. "A multiple-relaxation-time collision model by Hermite expansion." *Philosophical Transactions of the Royal Society A* 379, no. 2208 (2021): 20200406. <https://doi.org/10.1098/rsta.2020.0406>
- [10] Jonnalagadda, Anirudh, Atul Sharma, and Amit Agrawal. "Single relaxation time entropic lattice Boltzmann methods: A developer's perspective for stable and accurate simulations." *Computers & Fluids* 215 (2021): 104792. <https://doi.org/10.1016/j.compfluid.2020.104792>
- [11] Bhatnagar, Prabhu Lal, Eugene P. Gross, and Max Krook. "A model for collision processes in gases. I. Small amplitude processes in charged and neutral one-component systems." *Physical review* 94, no. 3 (1954): 511. <https://doi.org/10.1103/PhysRev.94.511>
- [12] Mahmoodi, Mostafa, and Seyed Mohammad Hashemi. "Numerical study of natural convection of a nanofluid in C-shaped enclosures." *International Journal of Thermal Sciences* 55 (2012): 76-89. <https://doi.org/10.1016/j.ijthermalsci.2012.01.002>



- 
- [13] Kamyar, A., Rahman Saidur, and M. Hasanuzzaman. "Application of computational fluid dynamics (CFD) for nanofluids." *International Journal of Heat and Mass Transfer* 55, no. 15-16 (2012): 4104-4115. <https://doi.org/10.1016/j.ijheatmasstransfer.2012.03.052>
- [14] Kefayati, G. H. R., S. F. Hosseinizadeh, M. Gorji, and H. Sajjadi. "Lattice Boltzmann simulation of natural convection in an open enclosure subjugated to water/copper nanofluid." *International Journal of Thermal Sciences* 52 (2012): 91-101. <https://doi.org/10.1016/j.ijthermalsci.2011.09.005>
- [15] Jonnalagadda, Anirudh, Atul Sharma, and Amit Agrawal. "Single relaxation time entropic lattice Boltzmann methods: A developer's perspective for stable and accurate simulations." *Computers & Fluids* 215 (2021): 104792. <https://doi.org/10.1016/j.compfluid.2020.104792>